

Effect of indented growth rings on spruce wood mechanical properties and subsequent violin dynamics

ROMAIN VIALA^{1,2}, JÉRÉMY CABARET¹, MARJAN SEDIGHI-GILANI³,
VINCENT PLACET⁴, SCOTT COGAN⁴

¹Institut Technologique Européen des Métiers de la Musique - ITEM, Le Mans, 72000, France,

²Laboratoire d'Acoustique de l'Université du Mans — LAUM CNRS 6613, 72085 Le Mans Cedex 09, France

³Swiss Federal Laboratories for Materials Science and Technology (EMPA), Überlandstrasse 129, CH-8600 Dübendorf, Switzerland

⁴Univ. Bourgogne Franche-Comté, FEMTO-ST Institute, CNRS/UFC/ENSMM/UTBM, Department of Applied Mechanics, 25000 Besançon, France

romain.viala@itemm.fr

January 18, 2024

Abstract

In this study, the influence of “bear claw” or indented growth ring anatomical patterns on the vibro-mechanical behavior of spruce wood have been investigated, particularly in the context of utilizing these singularities / specific features for the construction of violins. By employing vibrometry and modal analysis followed by finite element model updating, the vibro-mechanical properties (specific stiffness in longitudinal (L) and radial (R) directions and shear LR plane, and associated damping) of the indented growth rings spruce were identified and implemented in a numerical model of a violin. Results have revealed a significant increase in specific moduli in R direction and LR plane and decrease in L direction of spruce wood in the presence of indented growth rings, therefore accompanied by a reduction in anisotropic elastic properties, in comparison to spruce without these patterns. These properties led to changes in violin dynamics, globally increasing resonance frequencies and changing the shape of the vibration modes. The simulated frequency response function of the violin at the bridge suggested a global shift of the admittance of the bridge toward higher frequencies. These results suggest a potential impact of indented growth rings of spruce on the acoustic properties of instruments.

Keywords: Wood mechanics, Wood anatomy, Indented growth rings, Wood dynamics, Violin vibrations, Finite element model Updating

I. INTRODUCTION

It is a common belief of musicians, instrument makers and listeners that the finely selected wood that is used in musical instruments plays a prime role on the sound quality and timbre of the instrument. Instrument makers choose the wood used for musical instruments making based on various criteria including physical, mechanical, aesthetic, machinability, availability, habits. The presented work focuses on the specie used for the making of guitar and violin soundboards, spruce, *Picea abies*. It is usually considered that these woods are mainly selected for their mechanical properties, especially tonewood spruce that exhibits high specific rigidity along longitudinal axis. The wood anatomy in relation to its influence on the mechanical and acoustic properties of woods used for musical instruments has been a subject of investigations, associated with fiber waves Alkadri et al. (2018), interlocked grain Brémaud et al. (2010), extractives Brémaud et al. (2013) and grain angle Brémaud et al. (2011). In this context, the spruce wood (*Picea abies*) exhibiting

bear claw patterns or indented growth rings (IGR), known by their German name "*hazelfichte*" or "*épicéa chenillé*" or "*coudrier*" in French, emerges as a particularly interesting pattern due to its distinctively intricate and undulating grain patterns that evoke the imagery of marks left by claws or xylophagous insects. These patterns, which appear as convoluted lines and ripples on the wood surface, have interested luthiers, researchers, and musicians, igniting speculation about the potential implications of these unique anatomical features on the mechanical behavior of the wood and, by extension, on the dynamical response of musical instruments. Therefore, the interest for these patterns can be both aesthetic or mechanical.

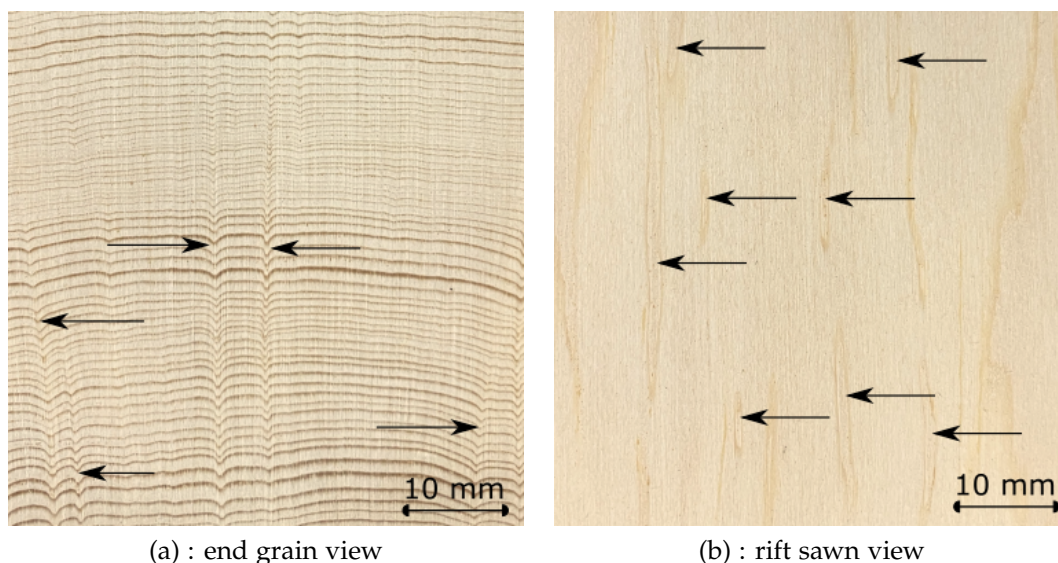
Wood shows a high variability in mechanical properties between different species, different subspecies, individuals and even inside the same individual. In Buksnowitz et al. (2007), it has been shown that the acoustical and mechanical properties of wood may not necessarily influence the instrument makers selection. Although smaller densities are observed for best ranked woods, the specific moduli, may be quite similar. Nevertheless, the wood used for instrument making is previously selected by the specialized vendor, and this selection is based on both objective and subjective assessments, among which the wood density and wave celerity, the straightness of the grain and the regularity of the annual rings can be keys to sort woods. Most of the time trunks showing nodes and irregular annual rings growth are rejected. The grain straightness is taken into consideration in the sorting process. The material properties of the wood as a function of the grading, and thus the price of the wood, have been barely studied Buksnowitz et al. (2007), Carlier et al. (2014), Viala et al. (2020). The works of Brémaud et al. (2011) and Bucur (1992) also sort the material properties of the tonewood for numerous samples using vibratory based tests. The specific studies, dedicated to spruce in general, have clustered a wide variety of experimental means, detailed below, and the differences observed according to the method have been studied in Sinclair & Farshad (1987) (excluding tonewoods). The different studies have led to the mean and standard deviation of spruce properties in all directions, reported in Brémaud et al. (2011). Spruce tonewood exhibits higher longitudinal modulus of elasticity E_L , lower longitudinal loss factor η_L , and higher anisotropy ratio between longitudinal and radial directions, $\frac{E_L}{E_R}$, compared to a spruce wood that has not been graded as tonewood Brémaud et al. (2012). In the same study it is also shown that there is a relation between damping and specific modulus of elasticity: an increase in the specific modulus leads to a decrease in loss factor following a linear relation between $\log(\eta_L)$ and $\log(\frac{E_L}{\rho})$, the specific modulus in longitudinal direction. In Haines (1980), it was observed that the stiffness of tonewoods is generally higher than the values reported for general woods. For decades, higher specific modulus has been considered as best choice for musical instruments Bucur (2016), and acoustic features based on a acoustic conversion efficiency (ACE) or radiation ratio (RR) have been proposed to sort woods used in musical instrument. In ?, the ACE was proposed as a way to maximize the peak response of a soundboard. The radiation ratio was also proposed as a way to increase the amplitude of the soundboard mobility and soundboard radiation. It has to be noted that the resulting sound of instruments is also dependent on other features of the instruments, such as f holes Nia et al. (2015). This relationship between geometrical features, material properties and resulting sound is more complex and less direct in chordophones compared to idiophones, as the produced sound is associated with a string and its characteristics and, the way to drive it. therefore, RR or ACE can be useful to compare wood but might not be sufficiently explicit to predict future sound of an instrument Chaigne & Kergomard (2008).

i. Indented Growth rings (IGR) and spruce properties

The spruce known as 'bear claw' exhibits a unique cellular arrangement that creates patterns resembling teeth of the annual rings in the radial-tangential (RT) plane, that can be as long as

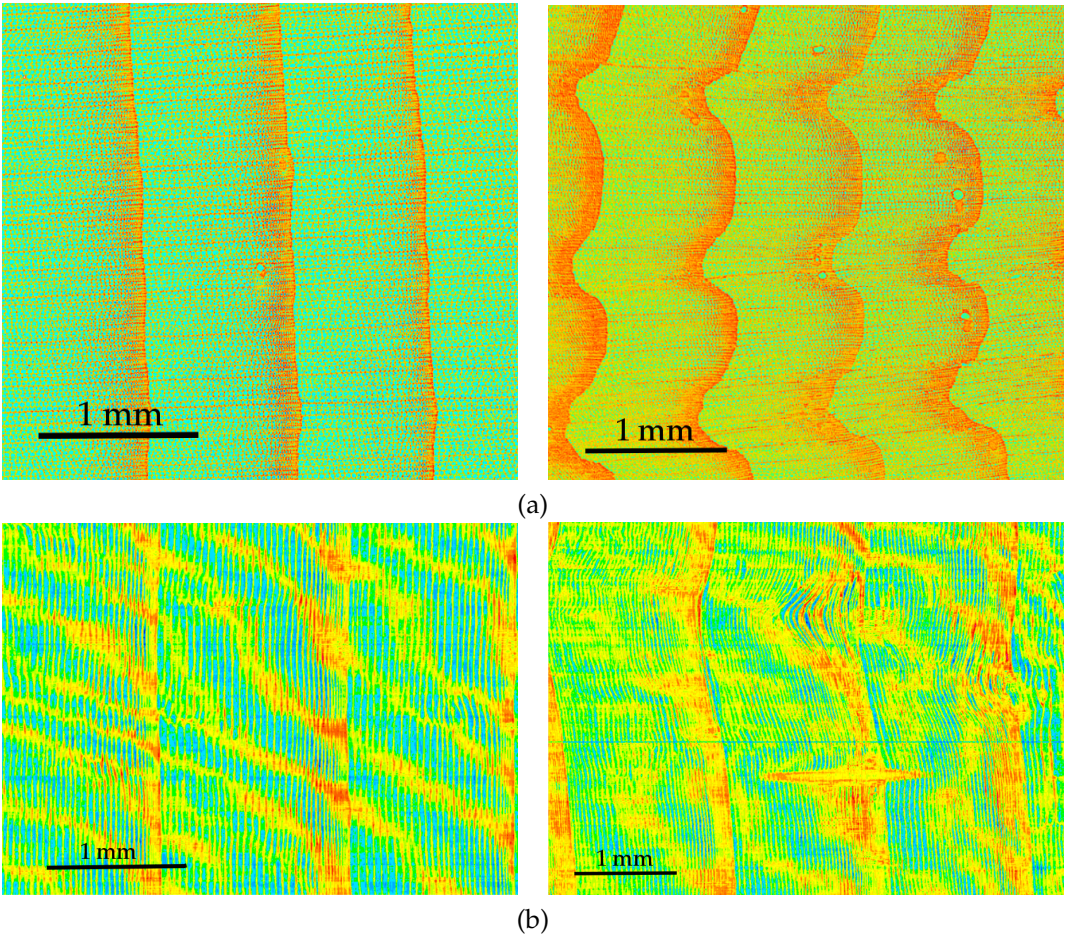
several centimeters in the longitudinal direction. These patterns, known as indented growth rings (IGR), are characterized by a sinuous interplay of light and dark lines, intricately woven into the wood's surface, creating a visual effect that has drawn the attention. The origin of these patterns remains a topic of speculation; some attribute them to genetic mutations or environmental influences during growth, while others propose that they are a result of damage or scratches in the cambium. In Račko et al. (2018), it has been proposed that fungal infection could be a potential explanation for the onset of annual growth rings during the juvenile phase, and that the disturbed zones originated in close proximity to leaf traces. More specifically, the IGR viewed from end grain plane, exhibit a pattern that may reproduce during many years, as shown in the Figure 1 (a). From another perspective, in the Figure 1 (b) in the LT plane, the IGR pattern are seen as long brown lines, whose lengths are several centimeters. Beyond their origins, IGR patterns have raised compelling questions about their potential influence on wood mechanical properties, making them an enticing subject for exploration. The Figure 2 shows a close-up using computed nanotomography, highlighting the difference between regular and IGR spruce in both RT (a) and LR (b) planes. Spruce with IGR seems to exhibit numerous resin canals (a, right) and more wavy tracheid ordering (b, right). The IGR patterns are clearly visible in the RT plane and the abnormal morphology and arrangement of tracheids and rays is visible in the longitudinal-radial (LR) plane in the Figure 2, (b). In Ohtani et al. (1987) the observations using scanning electron microscopy showed more trabeculae than for regular spruce and this effect was attributed to abnormal cell divisions.

Figure 1: Photographs of IGR spruce in RT plane (a) and LT plane (b). The arrows point to IGR patterns.



After a duration comprised between 20 to 50 years, the rings become normal again Schweingruber (2008). The same study showed that the number of rays is increased by up to 50 % in the IGR areas which may increase the stiffness in radial direction. The number of tracheids is only different in latewood, and their tangential diameter is higher in both earlywood and latewood. It has been shown that, in relation with cambial dynamics, the number of cells and the rings width is similar to normal wood Nocetti & Romagnoli (2008). Therefore, the cambial activity and the hormonal balance, may not be at the origin of this phenomenon. The scratching of the bark of *Pinus halepensis*, lead systematically to IGR for longitudinal scratches, the xylem

Figure 2: Microscopic views of IGR and regular spruce obtained by tomography reconstruction. The tomography has been performed by Marjan Gilani, at EMPA, and the reconstruction made by the author using Fiji software Schindelin et al. (2012).



formed exhibits distorted tracheids, more rays, narrow tracheids, but normal sized resin duct, produced two years after Lev-Yadun & Aloni (1991). From a mesoscopic and macroscopic point of view, the density of IGR spruce has been studied but the results of the different studies are not coherent. In Romagnoli et al. (2003), it is concluded that the presence of IGR induces an increase in density (+12.5 %), and that the effect is higher in earlywood (+14 %) than in latewood (+3 %). It has been shown in Racko & Cunderlik (2006) that the wood density was lower but very close, and that the maximum strength was lower for IGR spruce than for regular wood (67 and 76 MPa, respectively). In addition, the modulus of elasticity in the longitudinal direction was lower (8200 for IGR and 11900 MPa for regular, $p=0.1$ %). In contrast, Racko et al. (2014) showed that the density did not change significantly and the shear strength of IGR spruce was higher than for regular spruce. Another study, Buksnowitz et al. (2012), showed that the modulus of elasticity and maximum strength increases when IGR are present. Moreover, the anisotropy ratio between L and R directions of the maximum stress and modulus of elasticity decreased with IGR spruce. In Yaman (2007) the alignment and shape of tracheids irregular, distinctive trabeculae, multiseriate parenchym rays in addition to uniseriate rays were evaluated for Lebanon cedar (*Cedrus Libani* A. Rich). This may lead to increased E_R for the same density, namely a higher specific modulus in radial direction, and lower in longitudinal one. While the broader field of wood anatomy has contributed significantly to understanding the impact of IGR spruce patterns using microscopy and mechanical studies, the specific impact of such patterns on the dynamical behavior of musical instruments or its parts, especially within the context of instrument making, remains a relatively uncharted domain. The construction of musical instruments, especially those of the violin family, is meticulously performed and discussed and seeks to balance aesthetic, structural and acoustic considerations. Wood, being the primary material used in instrument crafting, is considered to play an important role in determining the timbre of the produced sound. Variations in wood anatomy, such as grain orientation, density, and anisotropy ratio of elastic properties, can impact the way sound waves travel through the material and interact with its structure. Some instrument makers are aware of this pattern, and, when carving soundboards with such type of spruce, they usually take into account this effect when carving wooden material (discussion with M. BEAUFORT, violin maker, Besançon, France). Nevertheless this aspect has not been extensively studied. The objective of this study is to investigate the interplay between IGR anatomical characteristics and the mechanical behavior of spruce wood used for musical instruments making, at the scale of wedges and in the frequency domain of musical instruments. Therefore the aim is to quantify how the presence of IGR influences key mechanical properties such as rigidity, damping and anisotropy ratio in L, R directions and LR plane of the quarter sawn wedges used for soundboard making. To achieve this, a multi-modal approach involving vibrometry, modal analysis, and finite element model updating to identify many properties at once is used, which is rarely applied in this field. Secondly, material properties of both regular and IGR spruce are implemented in the finite element model of a complete violin. The aim is to evaluate the impact on eigenfrequencies, eigenvectors and bridge admittance of the violin, which enables the evaluation of this effect only, all the other parameters remaining equal. This is a dedicated method to evaluate fine modifications, without making numerous instruments, a lengthy and costly experimental approach prevented by the variability of the materials and interfaces uncertainties, and geometrical tolerances, as shown in Viala et al. (2019). The methodology employed for mechanical evaluation and violin dynamics computations is presented in the next section detailing the sample preparation, experimental techniques, and numerical approaches. The results for each part of the work are then presented highlighting the observed changes for each observable of interest. Finally the implications of findings are discussed in the broader context of musical instrument construction and wood science.

II. MATERIAL AND METHODS

i. Studied materials

Regular and IGR spruce wood samples were selected by a wood seller and prepared according to the one shown in Viala et al. (2020). Fifteen spruce wedges were studied. The spruce wedges were labeled i varying from 1 to 15. The Table 1 gives the label of the wedges, their references, their harvest year, their specific gravity and their "grading" as sold by the sawmill. Seven samples exhibited IGR, described above, and eight could be considered as regular common spruce, *Picea abies*. The Figure 3 shows the average dimensions of the wedges and the directions in the orthotropic frame of wood material. The wood selection implied that growth rings width was evenly distributed along the wedges, although the spacing could vary between 0.8 and 1.5 mm depending on wedges, but this dimension was much smaller than the wavelength of bending waves below 4000 Hz (in 3.5 mm thickness plates in radial direction of spruce ($E_R \approx 1 \text{ GPa}, \rho \approx 440 \text{ kg.m}^{-3}$), equal to 50 mm. Therefore, despite the impact of annual rings average width on density and moduli, which was evaluated in the study, the local difference between annual growth rings was not of the order of magnitude of flexural waves. The sawmill that provided wood indicated that indented growth rings generally occurred on higher and older trees (at least 150 to 200 years), and generally on the last decades of the tree. Along the height, the phenomenon has been observed on the first log, up to 3 to 4 meters. The wood samples came from the forest of Jura mountains, close to the border between France and Switzerland. For all the wedges, the dimensions have been measured with a rule and a caliper. The precision of the length measured with the rule was $\pm 0.5 \text{ mm}$ and the precision of the trapezoidal shape, measured with a caliper was $\pm 0.1 \text{ mm}$. The samples were weighed with a KERN[®] weighing machine whose precision was $\pm 0.1 \text{ g}$. The average relative error on the evaluation of the mass was equal to $\pm 0.02 \%$. The volume was evaluated from the dimensions of the parts, as the hygroscopicity of the material prevented the use of Archimedes principle that might have led to sorption processes. The relative error on the estimation of the volume was estimated to $\pm 1.4 \%$. The density was evaluated with the ratio between the mass and the volume. The relative error on the evaluation of the density of the wedges was close to 1.5% . The parts were stored in a climatic chamber at 25°C 50% relative humidity until their mass exhibited variations lower than 0.1% during a week. After the study, cubic samples of wedges have been heated up to 103°C to be dehydrated and the moisture content has been evaluated, with an average value of $10 \pm 0.5 \%$, which is in accordance with the moisture content at equilibrium for spruce wood at 50% relative humidity Glass Samuel V.; & Zelinka (2010).

ii. Methods

Experimental set-up Acceleration measurements have been conducted on the IGR spruce violin wedges using an accelerometer (PCB 352A24) in free conditions (suspended in the top corners). The accelerometer, with a mass much lower than the wedge, was assumed to not affect the mechanical behaviour of the wedges. The wedge were acoustically excited by a 3" speaker near the bottom left of the wedge. The excitation signal was a swept sine ([100 - 5000 Hz]) and generated by the acquisition software (DANID¹) used to record the signals and also to compute the frequency Response Function (FRF) of the sample. In order to extract natural frequencies, mode shapes and damping ratios, ModAn² software has been used from the FRF performed by

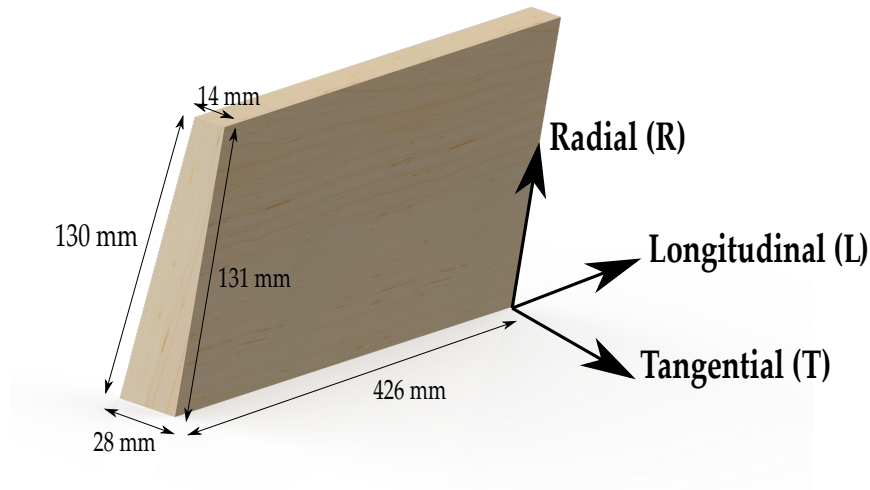
¹Danid software is developed by the Department of Applied Mechanics of the FEMTO-ST Institute

²The ModAn software is developed by the Department of Applied Mechanics Department of the FEMTO-ST Institute

Table 1: Spruce and maple violin wedges labels, references, harvest year, grading and specific gravity.

| Label | Reference | Year | Grading | Density ρ [$\frac{kg}{m^3}$] | Remarks | IGR surface density #/dm ² |
|-------|-----------|------|---------|-------------------------------------|---------|---------------------------------------|
| 1 | 10 Z 120 | 2010 | 1.A | 510 | - | - |
| 2 | 11 K 5 | 2011 | 1.A | 505 | IGR | 8 |
| 3 | 110 131 | 2011 | 1.A | 430 | IGR | 4 |
| 4 | 13 A3 60 | 2013 | 1.A | 460 | IGR | 3 |
| 5 | 10 Q 89 | 2010 | 1.B | 430 | - | - |
| 6 | 13 C 58 | 2013 | 1.B | 480 | - | - |
| 7 | 13 C 38 | 2013 | 1.B | 490 | - | - |
| 8 | WG 46 | 1996 | 2nd | 430 | IGR | 4 |
| 9 | WI 40 | 1998 | 2nd | 450 | - | - |
| 10 | WG 67 | 1996 | 2nd | 440 | IGR | 4 |
| 11 | 18 N 541 | 2018 | 1.A | 495 | IGR | 5 |
| 12 | 20 K 301 | 2020 | 1.A | 427 | - | - |
| 13 | 20 V 236 | 2020 | 1.A | 440 | - | - |
| 14 | 20 Z 366 | 2020 | 1.A | 436 | - | - |
| 15 | 21 A 123 | 2021 | 1.A | 436 | IGR | 5 |

Figure 3: Scheme of the average dimensions of the wedges and the directions in the orthotropic frame of wood material

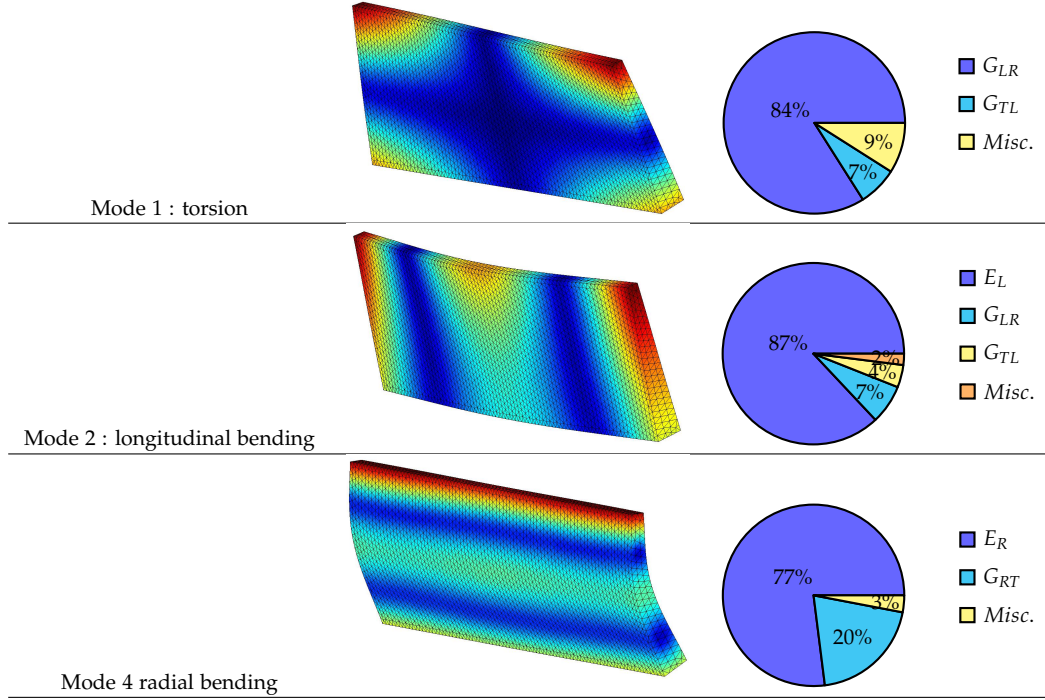


the acquisition software. Mechanical properties of the wedges were then estimated using a FEM model as explained in the next paragraph.

Material parameter identification with Finite Element Model Updating In Viala et al. (2020),
 180 Finite Element Model Updating (FEMU) has been used for the evaluation of spruce plates and
 wedges used for chordophones soundboard making. Three elastic parameters and three loss
 factors can be measured at once, showing difference according to the grading of the materials. A
 finite element model of the violin wedges was developed, incorporating actual geometries and
 orthotropic material properties. The model was iteratively updated using experimental modal
 185 data to optimize material parameters, and therefore identify the most accurate subset of material
 parameters. A finite difference sensitivity analysis based on frequencies showed in Viala et al.
 (2020) that E_L , E_R , G_{LR} , and their respective loss factors could be reliably identified. The Figure 4

shows examples of eigemodes of wedges and their respective sensitivity to material parameters, in which *misc.* refers to miscellaneous, gathering all the remaining elastic parameters except E_L , E_R and G_{LR} which are particularly influential, depending one the mode shape.

Figure 4: Mode shape (left) and screening of the parameters (right) according to their influence on each mode frequency. *Misc.* refers to miscellaneous, gathering all the remaining elastic parameters.



Along with the specific modulus in each directions, the radiation ratio RR_i is calculated for i directions as given in equation 1 and is associated with acoustic loudness.

$$RR_i = \sqrt{\frac{E_i}{\rho^3}} \quad (1)$$

. The acoustic conversion efficiency (ACE), in each direction, takes into account the corresponding loss factor the material, as given in equation 2. and can be associated with the acoustic peak responses Ono (1996), Wegst (2006).

$$ACE_i = \frac{RR_i}{\eta_i} \quad (2)$$

Finite Element Model of violin and outputs The computer aided design of the model was based on real wooden mould and jigs of an instrument maker of the earliest XXth century, Maurice Fauconnier. The rendered parametric computer aided design (CAD) of the violin is shown in the Figure 5 (a). A detailed numerical model has been constructed using the finite elements method based on the commercially available software MSC-PATRAN[®], shown on the Figure 5 (b). The mesh has been created using quadratic tetrahedral elements of 5 mm as global edge length, and orthotropic material parameters of the soundboard (upper plate) were defined based on the results of the identification campaign. The sides, neck and bridge were assumed to be made

of maple (*Acer pseudoplatanus*). For the fingerboard, chinrest, tailpiece and tuning pegs, ebony (*Diospyros crassiflora*) was considered. A modal analysis of the model has been performed in the frequency range from 1 to 4000 Hz, which has resulted in approximately hundreds of modes. The eigenfrequencies, eigenvectors (eigenmode shapes) and bridge admittance have been compared between a model with a soundboard with IGR spruce material properties and another one with regular spruce. The material parameters of the soundboard were taken from the results of the identification performed on wedges and the remaining parameters for maple, and ebony were taken from Viala (2018) and given in the table 2. The orientation of each solid according to the orientation of wood are represented in the Figure 6. The admittance of the bridge consists in the ratio between the output displacement on a point resulting from an input force as a function of the frequency. It is a frequency response function based on the modal superposition method. This synthesis needs the modal damping of each mode to be performed. For this study, the modal damping was based on the modal damping evaluated with the data of real violins given in Viala (2018), and close to 1 %. Once the modal basis of the full mounted violin was computed and the bridge admittance was computed at the point shown in Figure 7. The eigenmodes of modal basis of both regular and IGR spruce soundboard have been compared. The eigenmodes were correlated with a modal assurance criterion (MAC) Allemang & Brown (1982), a scalar between 0 and 1 for each mode indicating the proximity between each modal bases, with 1 indicating identical mode shapes. Considering the main changes that can happen between two numerical cases and the sensitivity of the MAC criterion, this allowed the matching of many modes between two differing modal bases. The matched eigenfrequency errors (M.E.E.) were used to study the impact of IGR on the eigenfrequency of each mode that was computed. The matched eigenvector error associated with the MAC number were used to compare the deformed shape) of a given mode of a modal basis with another one.

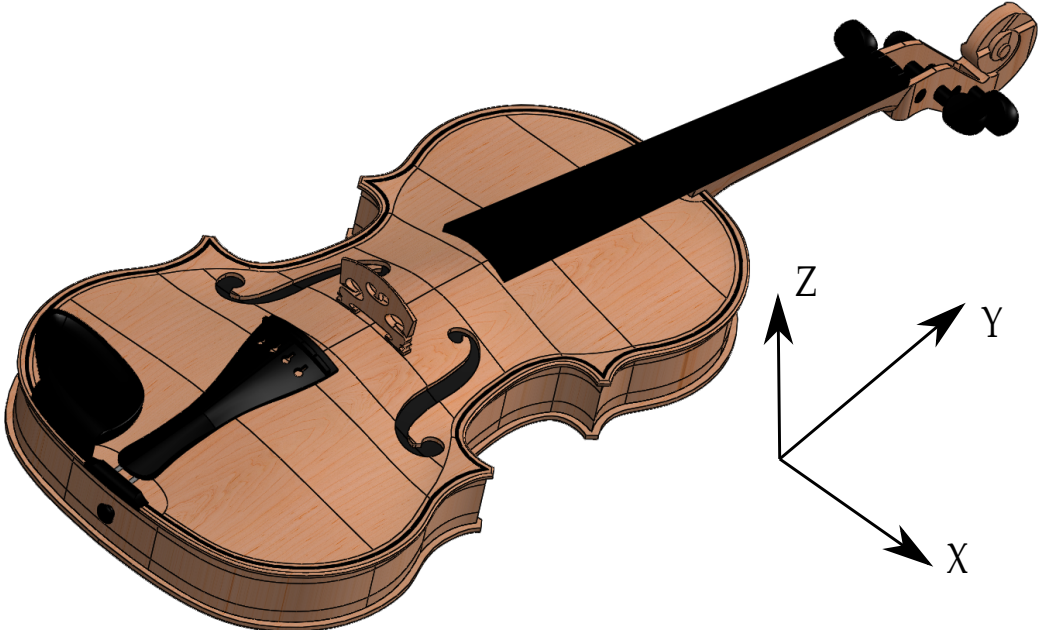
Table 2: Material properties values used for maple and ebony parts. The values for ebony are taken from Guitard & El Amri (1987) and the results for maple are taken from Viala (2018), Viala et al. (2020).

| Ebony (<i>Diospyros Crassiflora</i>) | | Maple (<i>Acer pseudoplatanus</i>) | |
|--|-------|--------------------------------------|-------|
| Material parameter | Value | Material parameter | Value |
| E_L (MPa) | 17000 | E_L (MPa) | 14920 |
| E_R (MPa) | 1960 | E_R (MPa) | 1960 |
| E_T (MPa) | 1110 | E_T (MPa) | 1110 |
| ν_{LR} | 0.37 | ν_{LR} | 0.37 |
| ν_{RT} | 0.65 | ν_{RT} | 0.65 |
| ν_{TL} | 0.032 | ν_{TL} | 0.032 |
| G_{LR} (MPa) | 1370 | G_{LR} (MPa) | 1370 |
| G_{RT} (MPa) | 360 | G_{RT} (MPa) | 360 |
| G_{TL} (MPa) | 950 | G_{TL} (MPa) | 950 |
| ρ (g/cm ³) | 1 | ρ (g/cm ³) | 0.64 |

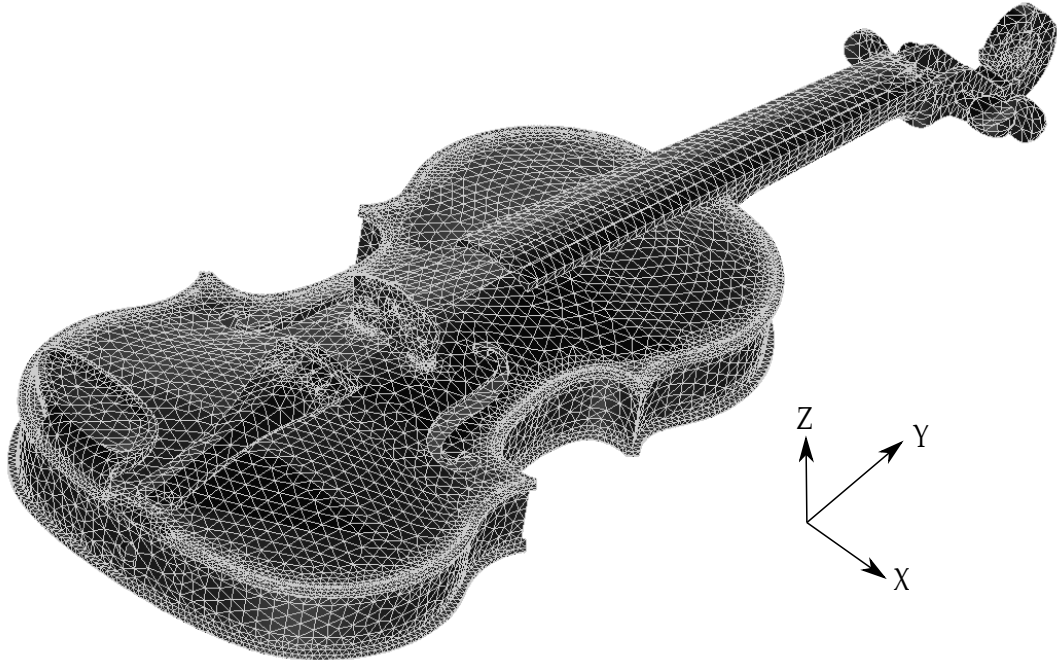
III. RESULTS

The identified properties of the wedges are given in the tables 3 and 4. The specific gravity mean value is equal to 0.46. The averaged values of the moduli in L and R directions are equal to 13.7 and 1.7 GPa, respectively. The loss factors in the same directions are equal to 0.75 and 1.8 %, respectively. In the LR plane the average value of the shear modulus is equal to 0.9 GPa, and the loss factor in this plane is equal to 1.3 %. The corresponding specific parameters are given in the table 4, such parameters are more interesting for the dynamical behavior as they are intrinsically associated with the speed of flexural waves, along with thickness and frequency of plate-like parts.

Figure 5: (a) Computer aided designs of the violin ; (b) Tetrahedral meshing of the violin.



(a)

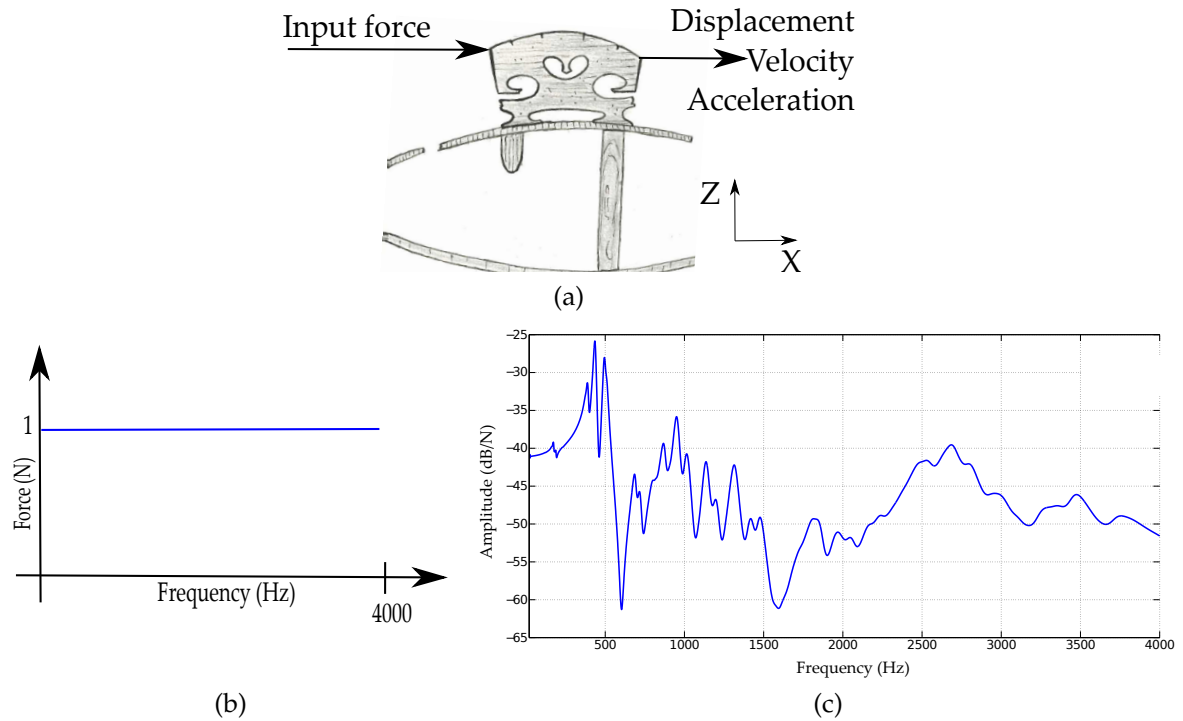


(b)

Figure 6: Scheme of the material orientation of the parts in the violin.



Figure 7: (a) Bridge admittance evaluation scheme ; (b), input force as a function of frequency; (c), computed FRF at the bridge on full violin model with nominal parameters.



The averaged values of the specific Young's moduli in L and R directions are equal to 30 and 3 GPa, respectively. In the LR plane the specific shear modulus averaged value is equal to 1.8 GPa.

Table 3: Identified material properties for spruce wedge samples and associated average and coefficient of variation.

| Sample | Grad. | Ref. | Density [$\frac{kg}{m^3}$] | Remarks | E_L (GPa) | E_R (GPa) | G_{LR} (GPa) | η_L (%) | η_R (%) | η_{LR} (%) | Anisotropy $\frac{E_L}{E_R}$ |
|----------------|-------|----------|---------------------------------|------------|----------------|----------------|-------------------|-----------------|-----------------|--------------------|------------------------------|
| 1 | 1.A | 10Z120 | 506 | - | 16.2 | 1.55 | 0.75 | 0.92 | 1.90 | 1.54 | 10.45 |
| 2 | 1.A | 11K5 | 505 | IGR | 13.6 | 1.93 | 1.19 | 0.74 | 1.48 | 1.38 | 7.05 |
| 3 | 1.A | 110131 | 430 | IGR | 12.1 | 1.05 | 0.57 | 0.74 | 1.76 | 1.44 | 11.5 |
| 4 | 1.A | 13A360 | 460 | IGR | 15.9 | 1.36 | 0.89 | 0.68 | 2.20 | 1.34 | 11.7 |
| 5 | 1.B | 10Q89 | 430 | - | 13.4 | 0.97 | 0.60 | 0.74 | 1.82 | 1.38 | 13.81 |
| 6 | 1.B | 13C58 | 480 | - | 16.0 | 1.24 | 0.82 | 0.68 | 2.0 | 1.34 | 12.9 |
| 7 | 1.B | 13C38 | 490 | - | 14.4 | 1.14 | 0.94 | 0.72 | 1.66 | 1.30 | 12.6 |
| 8 | 2nd | 96WG46 | 430 | IGR | 9.0 | 1.34 | 0.83 | 0.76 | 1.42 | 1.10 | 6.7 |
| 9 | 2nd | 98WI40 | 450 | - | 14.2 | 0.83 | 0.72 | 0.70 | 1.74 | 1.24 | 17.1 |
| 10 | 2nd | 96WG67 | 440 | IGR | 11.8 | 1.53 | 0.87 | 0.76 | 1.42 | 1.26 | 7.7 |
| 11 | 1.A | 18 N 541 | 495 | IGR | 15.1 | 2.85 | 1.14 | 0.76 | 1.94 | 1.38 | 5.3 |
| 12 | 1.A | 20 K 301 | 427 | - | 13.4 | 1 | 0.73 | 0.76 | 1.78 | 1.34 | 13.4 |
| 13 | 1.A | 20 V 236 | 440 | - | 14.2 | 1.06 | 0.73 | 0.74 | 1.8 | 1.54 | 13.4 |
| 14 | 1.A | 20 Z 366 | 436 | - | 13.7 | 0.99 | 0.72 | 0.76 | 1.86 | 1.38 | 13.8 |
| 15 | 1.A | 21 A 123 | 436 | IGR | 13.0 | 2.04 | 0.84 | 0.78 | 2 | 1.4 | 6.4 |
| Average | - | - | 460 | - | 13.7 | 1.7 | 0.9 | 0.75 | 1.78 | 1.34 | 10.9 |
| COV [%] | - | - | 6 | - | 13 | 39 | 21 | 4 | 13 | 7 | 33 |

Table 4: Specific moduli, density and anisotropy for wedge samples.

| Sample | Density ρ [$\frac{kg}{m^3}$] | Remark | $\frac{E_L}{\rho}$ [GPa.cm ³ .g ⁻¹] | $\frac{E_R}{\rho}$ [GPa.cm ³ .g ⁻¹] | $\frac{C_{LR}}{\rho}$ [GPa.cm ³ .g ⁻¹] |
|----------------|--|------------|---|---|--|
| 1a | 506 | - | 32.0 | 3.06 | 1.49 |
| 2a | 505 | IGR | 26.9 | 3.82 | 2.37 |
| 3a | 43 | IGR | 28.2 | 2.45 | 1.34 |
| 4a | 460 | IGR | 34.5 | 2.94 | 1.92 |
| 5a | 430 | - | 31.0 | 2.24 | 1.40 |
| 6a | 480 | - | 33.2 | 2.58 | 1.71 |
| 7a | 490 | - | 29.5 | 2.33 | 2.7 |
| 8a | 430 | IGR | 20.7 | 3.09 | 2.10 |
| 9a | 450 | - | 31.4 | 1.84 | 1.60 |
| 10a | 440 | IGR | 26.9 | 3.5 | 1.99 |
| 11a | 495 | IGR | 30.5 | 5.8 | 2.3 |
| 12a | 427 | - | 31.4 | 2.3 | 1.7 |
| 13a | 440 | - | 32.3 | 2.4 | 1.65 |
| 14a | 436 | - | 31.3 | 2.3 | 1.65 |
| 15a | 436 | IGR | 29.8 | 4.7 | 1.95 |
| Average | 457 | - | 30.0 | 3.0 | 1.8 |
| COV [%] | 6 | - | 11 | 36 | 16 |

Table 5: Radiation ratios and acoustic conversion efficiency for different directions of wedge samples and associated average and coefficient of variation (COV)

| Sample | RR_L [$\frac{m^4}{kg.s}$] | RR_R [$\frac{m^4}{kg.s}$] | RR_{LR} [$\frac{m^4}{kg.s}$] | ACE_L [$\frac{m^4}{kg.s}$] | ACE_R [$\frac{m^4}{kg.s}$] | ACE_{LR} [$\frac{m^4}{kg.s}$] |
|----------------|----------------------------------|----------------------------------|-------------------------------------|-----------------------------------|-----------------------------------|--------------------------------------|
| 1a | 11.2 | 3.5 | 2.4 | 1215 | 182 | 156 |
| 2a | 10.3 | 3.9 | 3.0 | 1389 | 262 | 220 |
| 3a | 12.3 | 3.6 | 2.7 | 1667 | 206 | 186 |
| 4a | 12.8 | 3.7 | 3.0 | 1880 | 170 | 226 |
| 5a | 13.0 | 3.5 | 2.7 | 1754 | 192 | 199 |
| 6a | 12.0 | 3.35 | 2.7 | 1769 | 167 | 203 |
| 7a | 11.1 | 3.1 | 2.8 | 1537 | 188 | 217 |
| 8a | 10.6 | 4.1 | 3.2 | 1400 | 289 | 294 |
| 9a | 12.5 | 3.0 | 2.8 | 1783 | 173 | 227 |
| 10a | 11.8 | 4.2 | 3.2 | 1549 | 298 | 254 |
| 11a | 11.2 | 4.8 | 3.1 | 1468 | 250 | 222 |
| 12a | 13.1 | 3.6 | 3.1 | 1726 | 201 | 229 |
| 13a | 12.91 | 3.5 | 2.9 | 1745 | 196 | 190 |
| 14a | 12.9 | 3.5 | 2.9 | 1692 | 186 | 214 |
| 15a | 12.5 | 5.0 | 3.2 | 1606 | 248 | 227 |
| Average | 12 | 3.8 | 2.9 | 1611 | 214 | 218 |
| COV [%] | 8 | 15 | 6 | 9 | 21 | 12 |

i. Regular and IGR spruce comparison

The analysis of IGR spruce violin wedges revealed a statistically significant increase in specific radial and small decrease in longitudinal moduli compared to traditional spruce. The comparison of the material properties between regular and IGR spruce are given in the table 6. The specific gravity of the regular spruce and IGR one were close. In Racko & Cunderlik (2006) the density was higher and lower in Romagnoli et al. (2003), therefore results were consistent with usual observations, depending on sampling. For the comparison, only the specific parameters were considered, to avoid the correlation between the mechanical properties and the density. The most important variation concerned the specific modulus in the R direction, higher for IGR spruce specimens ($3.75 [GPa.cm^3.g^{-1}]$) than for regular ones ($2.4 [GPa.cm^3.g^{-1}]$), which was expected according to Buksnowitz et al. (2012) possibly associated with multiseriate parenchym rays in addition to uniseriate rays. In this paper, the IGR were associated with a significant decrease of the anisotropy of spruce. Based on the presented results, the anisotropy fell from 13.4 (regular) to 8 (IGR). The specific Young's modulus in L direction was higher for regular specimens ($31.5 [GPa.cm^3.g^{-1}]$) than for the IGR ones ($28.2 [GPa.cm^3.g^{-1}]$), which was in accordance with Racko & Cunderlik (2006). The specific shear modulus in LR plane was smaller for regular specimens ($1.6 [GPa.cm^3.g^{-1}]$) than for IGR ones ($2 [GPa.cm^3.g^{-1}]$). The results were significant for E_R , $\frac{E_R}{\rho}$, $\frac{C_{LR}}{\rho}$ and *Anisotropy* especially, and to a lower extent for $\frac{E_L}{\rho}$. Considering outputs more related to the acoustic properties of wood, results showed a significant impact of IGR on radiation ratios in R direction and in LR plane, suggesting an higher loudness for sound produced by vibratory response, yet hard to quantify in the case of chordophones where the response is associated with the dynamics of the strings attached on the instrument. Results also showed a significant impact on acoustic conversion efficiency (from 186 to 246 [$\frac{m^4}{kg.s}$]), which, since the loss factors between each population were similar, was expected. This suggested higher values of the amplitude of frequency response peaks in case of dynamical comparison between specimens exhibiting IGR or not, and frequency response functions of a violin for modes driving the soundboard. But this effect was countered by the decrease of acoustic conversion efficiency in longitudinal direction (from 1653 to 1565 [$\frac{m^4}{kg.s}$]). Therefore, except for modes driving the soundboard only in radial direction, such effect would presumably be hard to evaluate on the bridge admittance for example, which was confirmed by dynamical results.

ii. Effect of IGR spruce on violin dynamics

The results of the previous section have been implemented in the violin model, changing only mechanical parameters of the soundboard, all the other material parameters remaining the same, which enabled a comparison of the impact of IGR only. The Figure 8 shows three vibratory modes of the signature response of the violins, namely CBR, B1- and B1+, and their respective usual experimental ranges Elie (2012). Results showed an increase in frequency for soundboards with IGR spruce, from 2 to 4 % depending on the modes. Those modes are driving the soundboard in longitudinal and radial way, which implies that changes in radial and longitudinal stiffness of wood have an impact on their frequencies. The table 7 gives the compared eigenvalues and eigenmodes shapes using MAC criterion. The MAC matrix is shown in the Figure 10. The average criterion decreased to 80 % up to 4000 Hz, showing changes in mode shapes, which is a coherent result with the drop of anisotropy. The effect was increased above 1500 Hz (modes number above 30), which is considered as the medium frequencies range for violins Viala (2018). Nevertheless, the averaged matched eigenfrequency difference was equal to 2.7 % showing lower impact on mode

Table 6: Comparison of the mechanical properties between normal spruce and IGR spruce. The T statistic is calculated for bilateral distribution type and heteroscedastic distributions.

| Parameter | Regular | IGR | t-statistic |
|---|-------------|-------------|---------------|
| Density ρ [$\frac{kg}{m^3}$] | 457 ± 30 | 457 ± 31 | 0.96 |
| E_L [GPa] | 14.4 ± 1.1 | 12.9 ± 2.3 | 0.15 |
| E_R [GPa] | 1.1 ± 0.2 | 1.7 ± 0.6 | 0.03 |
| G_{LR} [GPa] | 0.75 ± 0.1 | 0.9 ± 0.2 | 0.11 |
| η_L [%] | 0.75 ± 0.07 | 0.75 ± 0.03 | 0.82 |
| η_R [%] | 1.82 ± 0.1 | 1.75 ± 0.3 | 0.57 |
| η_{LR} [%] | 1.38 ± 0.1 | 1.33 ± 0.11 | 0.37 |
| $\frac{E_L}{\rho}$ [$GPa.cm^3.g^{-1}$] | 31.5 ± 1.1 | 28.2 ± 4.2 | 0.08 |
| $\frac{E_R}{\rho}$ [$GPa.cm^3.g^{-1}$] | 2.4 ± 0.35 | 3.75 ± 1.1 | 0.02 |
| $\frac{G_{LR}}{\rho}$ [$GPa.cm^3.g^{-1}$] | 1.65 ± 0.16 | 2.0 ± 0.35 | 0.05 |
| Anisotropy $\frac{E_L}{E_R}$ [-] | 13.4 ± 1.8 | 8.0 ± 2.5 | 0.0007 |
| RR_L [$\frac{m^4}{kg.s}$] | 12.3 ± 0.8 | 11.6±1 | 0.16 |
| RR_R [$\frac{m^4}{kg.s}$] | 3.4± 0.2 | 4.2±0.5 | 0.005 |
| RR_{LR} [$\frac{m^4}{kg.s}$] | 2.8 ± 0.2 | 3.0 ± 0.2 | 0.025 |
| ACE_L [$\frac{m^4}{kg.s}$] | 1653±193 | 1565±172 | 0.37 |
| ACE_R [$\frac{m^4}{kg.s}$] | 186±11.3 | 246±45 | 0.01 |
| ACE_{LR} [$\frac{m^4}{kg.s}$] | 204±24 | 233±34 | 0.08 |

frequencies rather than on mode shapes. The bridge admittance with models whose soundboards are either made of IGR or regular wood are displayed in the Figure 9. According to results, the IGR wood anatomic feature tends to stiffen the soundboard for equivalent mass, and the FRF was slightly offset to the high frequencies. This indicated a possible impact on dynamical behaviour of the instrument for geometry remaining the same, and suggested a sufficient impact to be measured above the repeatability of dynamical measurements, generally close for the frequencies evaluation to 1 % due to geometric tolerances Viala et al. (2019). Nevertheless, the amplitude of the peaks was not particularly affected, which was partly expected considering the increase in ACE_R and, at the same time, the decrease in ACE_L which led to antagonist effects. Moreover, between 2000 and 3000 Hz, a general shift towards high frequencies of the global shape of the admittance, consisting in a broad peak called the bridge hill effect Woodhouse (2005), Jansson & Barczewski (2016) was observed. The characteristics of the bridge hill effect are associated with the geometry of the bridge of the violin and its interaction with the soundboard, which in this study had an impact through the increase in specific radial modulus.

IV. DISCUSSION

The spruce specimens presenting IGR showed $\frac{E_R}{d\rho} \frac{G_{LR}}{\rho}$ values that are systematically higher than the regular ones and lower for $\frac{E_L}{\rho}$. Moreover, no particular changes on the density have been observed and the anisotropy has been considerably reduced, which is in accordance with the dedicated studies. The IGR patterns led to a wooden material with increased stiffness, radiation ratio and acoustic conversion efficiency in radial direction for equivalent density. This observation would be, at least partly, explained with an higher amount of rays (mesoscopic scale) or higher MFA (microscopic scale) in IGR patterns wood. Moreover, the grain deviation in these area can be a contribution of longitudinal stiffness into the radial one. The results therefore have demonstrated that selecting IGR wood would imply different mechanical properties, especially in violins where

Figure 8: Three canonical numerical modes of the violin body. Reference values are given from Hutchins & Voskuil (1993) and Gough (2013)

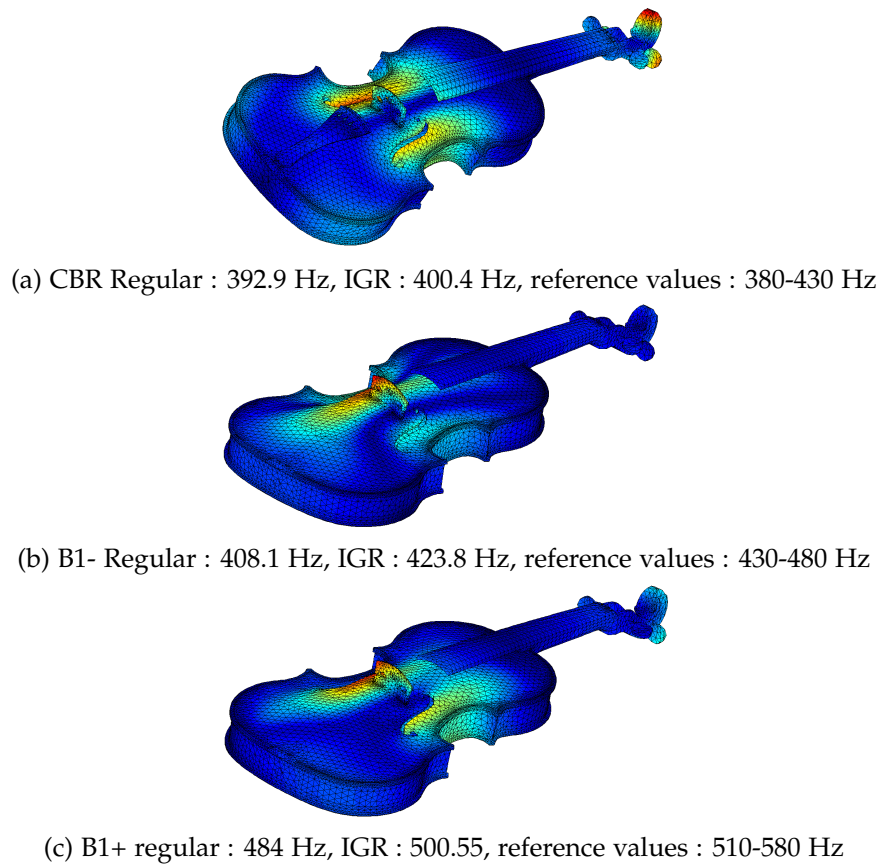


Figure 9: Violin bridge admittance compared between IGR and regular wood

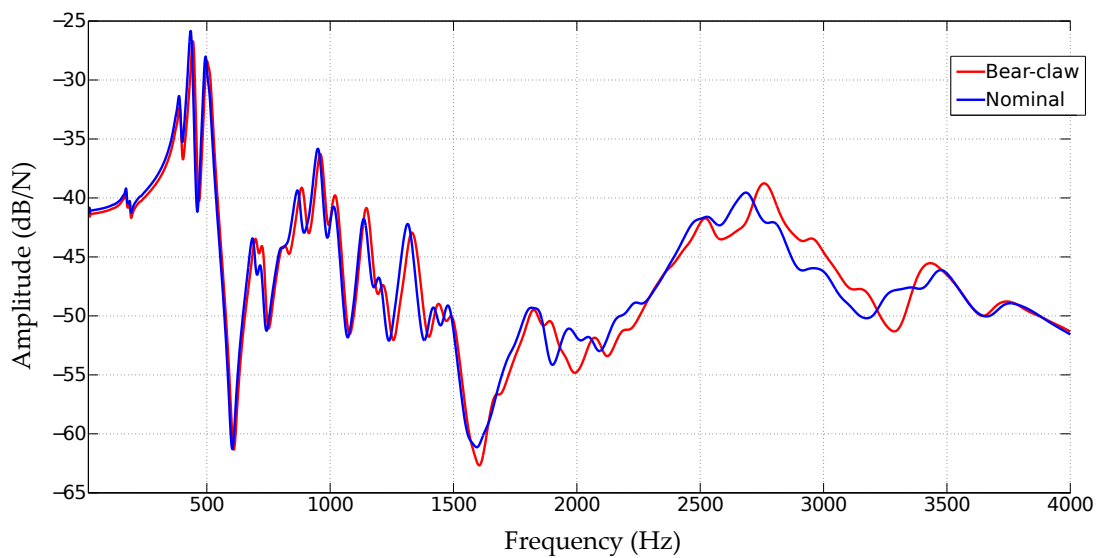
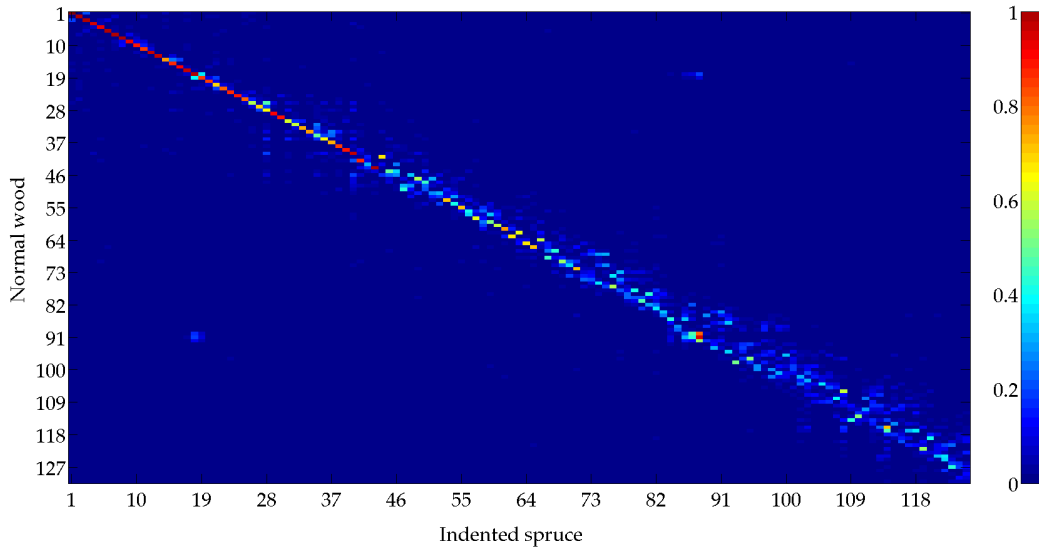


Table 7: Comparison between IGR and regular spruce soundboard on the computed modal bases eigenfrequencies and eigenvectors.

| IGR spruce soundboard | | Regular spruce soundboard | | M.E.E. (%) | MAC (%) |
|-----------------------|----------------|---------------------------|----------------|-------------|-------------|
| Mode | Frequency (Hz) | Mode | Frequency (Hz) | | |
| 1 | 197.55 | 1 | 194.97 | -1.31 | 100 |
| 2 | 248.39 | 2 | 245.89 | -1 | 100 |
| 3 | 299.58 | 3 | 298.09 | -0.5 | 99.8 |
| 4 | 400.37 | 4 | 392.94 | 1.86 | 94.5 |
| 5 | 423.81 | 5 | 408.15 | 3.69 | 92.1 |
| 6 | 500.55 | 6 | 484.06 | 3.3 | 99.4 |
| 7 | 544.9 | 7 | 541.48 | 0.63 | 99.2 |
| 8 | 591.53 | 8 | 588.1 | 0.58 | 99.8 |
| 9 | 658.78 | 9 | 637.43 | 3.24 | 92.5 |
| 10 | 670.66 | 10 | 650.96 | 2.94 | 89.2 |
| 11 | 701.98 | 11 | 689.93 | 1.72 | 84.1 |
| 12 | 738.28 | 12 | 719.41 | 2.56 | 97.5 |
| 13 | 762.09 | 13 | 724 | 5 | 96.4 |
| 14 | 809.92 | 14 | 796.99 | 1.6 | 74.4 |
| 15 | 811.66 | 15 | 801.28 | 1.28 | 87.7 |
| 16 | 858.3 | 16 | 824.71 | 3.91 | 91.6 |
| 17 | 929.32 | 17 | 913.08 | 1.75 | 97.9 |
| 18 | 965.41 | 18 | 964.08 | 0.14 | 99.8 |
| 19 | 981.48 | 19 | 977.92 | 0.36 | 85.4 |
| 20 | 1044 | 20 | 991 | 5.08 | 85.8 |
| 21 | 1069.94 | 21 | 1046.73 | 2.17 | 68.5 |
| 22 | 1102.16 | 22 | 1059.92 | 3.83 | 81.4 |
| 23 | 1153.8 | 23 | 1117.25 | 3.17 | 87.6 |
| 24 | 1198.44 | 24 | 1163.76 | 2.89 | 89.8 |
| 25 | 1249.92 | 25 | 1226.76 | 1.85 | 80.1 |
| 26 | 1283.4 | 26 | 1249.93 | 2.61 | 56.2 |
| 27 | 1314.54 | 27 | 1274.86 | 3.02 | 68.6 |
| 28 | 1333.87 | 28 | 1292.98 | 3.07 | 64.4 |
| 29 | 1368.39 | 29 | 1338.57 | 2.18 | 90.1 |
| 30 | 1436.26 | 30 | 1371.27 | 4.52 | 89.1 |
| 31 | 1485.38 | 31 | 1413.9 | 4.81 | 60.2 |
| 32 | 1497.84 | 32 | 1439.31 | 3.91 | 58.2 |
| 33 | 1516.56 | 33 | 1472.5 | 2.91 | 73.2 |
| 34 | 1547.7 | 34 | 1505.05 | 2.76 | 74.2 |
| 35 | 1559.13 | 35 | 1507.47 | 3.31 | 48.5 |
| 36 | 1577.96 | 36 | 1524.33 | 3.4 | 65.9 |
| 37 | 1605.32 | 37 | 1568.5 | 2.29 | 72.1 |
| 38 | 1623.14 | 38 | 1606.39 | 1.03 | 85.2 |
| 39 | 1649.37 | 39 | 1633.55 | 0.96 | 88.2 |
| 40 | 1722.87 | 40 | 1691.26 | 1.83 | 96.8 |
| 41 | 1789.79 | 42 | 1741.56 | 2.69 | 86.2 |
| 42 | 1811.65 | 43 | 1783.66 | 1.55 | 31.3 |
| 43 | 1826.04 | 44 | 1823.92 | 0.12 | 99.1 |
| 44 | 1845.56 | 41 | 1724.17 | 6.58 | 66.8 |
| 45 | 1899.91 | 45 | 1831.04 | 3.62 | 49.1 |
| 47 | 1945.03 | 50 | 1927.2 | 0.92 | 43.2 |
| 48 | 1964.68 | 46 | 1836.02 | 6.55 | 32.6 |
| 49 | 1971.97 | 47 | 1886.89 | 4.31 | 57.4 |
| 50 | 2002.65 | 48 | 1890.19 | 5.62 | 46 |
| Average: | | | | 2.7 | 79 |

Figure 10: MAC matrix between modal basis nominal and IGR spruce up to 4000 Hz.



R direction and shear LR plane properties also impact the dynamical behavior of the instrument Viala et al. (2016). The results on the model of violin showed a stiffening effect and therefore higher resonant frequencies, and different eigenmode shapes above 1500 Hz. This findings suggest that for a given geometry, violins made with regular or IGR spruce may exhibit different behavior. This was also legible with a broader output, the bridge hill of the violin, where the large peak showed a shift toward higher frequencies on an area often studied in acoustics of the violin.

V. CONCLUSION

This study revealed a significant impact of IGR on the mechanical parameters of spruce wood used for soundboards. This was correlated with a notable reduction in the anisotropy ratio of stiffness L and R within the spruce wood. This reduction indicated a more uniform distribution of mechanical properties across different directions. The difference led to modifications in the violin dynamics, increasing resonance frequencies and changing the shape of the vibration modes. These findings have direct implications for the construction of violins and wedges selection, where the unique properties of IGR spruce may impact acoustic properties. Future researches could delve into the intricate micro structure of IGR patterns and their impact on wood mechanics. Moreover, a perspective would be to study this effect on the dynamics of the violin, considering the makers tolerance on the geometry of the violin. This type of study would require a high number of instruments to be statistically demonstrated, as shown in Viala et al. (2019). Therefore the numerical models based on finite element method may be particularly relevant to study phenomena with high variability, in models where only one parameter can be changed at a time. Finally, another important future topic would be the demonstration that significantly different dynamical behavior may be heard or perceived by the musician or listener in playing conditions as performed in Fritz et al. (2012). This is generally hard to achieve since the characteristics of the strings and their actuation are of prime order and hardly repeatable. To this end, models can also be used to compute sound and therefore provide acoustic comparison of violins, one step beyond their dynamical behaviour consisting in resonant frequencies or frequency response functions.

REFERENCES

- Alkadri, A., Carlier, C., Wahyudi, I., Gril, J., Langbour, P. & Brémaud, I. (2018), 'Relationships
335 between anatomical and vibrational properties of wavy sycamore maple', *IAWA Journal* **39**(1), 63–86.
URL: <http://booksandjournals.brillonline.com/content/journals/10.1163/22941932-20170185>
- Allemang, R. J. & Brown, D. L. (1982), A correlation coefficient for modal vector analysis, in 'First International Modal Analysis Conference', Orlando, pp. 110–116.
- 340 Brémaud, I., Amusant, N., Minato, K., Gril, J., Brémaud, I., Amusant, N., Minato, K., Gril, J., Thibaut, B., Brémaud, I., Amusant, N., Minato, K., Gril, J. & Thibaut, B. (2013), 'Effect of extractives on vibrational properties of African Padauk (*Pterocarpus soyauxii* Taub .) To cite this version : HAL Id : hal-00804236 Effect of extractives on vibrational properties of African Padauk (*Pterocarpus soyauxii* Taub .)'.
URL: <https://hal.archives-ouvertes.fr/hal-00804236>
- 345 Brémaud, I., Cabrolhier, P., Gril, J., Clair, B., Gérard, J., Minato, K. & Thibaut, B. (2010), 'Identification of anisotropic vibrational properties of Padauk wood with interlocked grain', *Wood Science and Technology* **44**(3), 355–367.
- Brémaud, I., El Kaïm, Y., Guibal, D., Minato, K., Thibaut, B. & Gril, J. (2012), 'Characterisation and categorisation of the diversity in viscoelastic vibrational properties between 98 wood types',
350 *Annals of Forest Science* **69**(3), 373–386.
URL: <http://link.springer.com/10.1007/s13595-011-0166-z>
- Brémaud, I., Gril, J. & Thibaut, B. (2011), 'Anisotropy of wood vibrational properties: Dependence on grain angle and review of literature data', *Wood Science and Technology* **45**(4), 735–754.
- Bucur, V. (1992), 'Le Bois de Lutherie', *Journal de physique IV* **02**, 8.
- 355 Bucur, V. (2016), *Handbook of Materials for String Musical Instruments*.
- Buksnowitz, C., Evans, R., Müller, U. & Teischinger, A. (2012), 'Indented rings (hazel growth) of Norway spruce reduce anisotropy of mechanical properties', *Wood Science and Technology* **46**(6), 1239–1246.
URL: <http://link.springer.com/10.1007/s00226-012-0480-0>
- 360 Buksnowitz, C., Teischinger, A., Müller, U., Pahler, A. & Evans, R. (2007), 'Resonance wood [Picea abies] -evaluation and prediction of violin makers' quality-grading.', *The Journal of the Acoustical Society of America* **121**(4), 2384–2395.
- Carlier, C., Brémaud, I. & Gril, J. (2014), Violin making " tonewood ": comparing makers ' empirical expertise with wood structural / visual and acoustical properties, in 'Symposium on Musical
365 Acoustics ISMA2014', Le Mans, pp. 325–330.
- Chaigne, A. & Kergomard, J. (2008), *Acoustique des instruments de musique*, Belin.
URL: <https://hal.archives-ouvertes.fr/hal-00871263>
- Elie, B. (2012), Caractérisation vibratoire et acoustique des instruments à cordes, PhD thesis, Université du Maine.
370 URL: <http://tel.archives-ouvertes.fr/tel-00833885/>

- Fritz, C., Curtin, J., Poitevineau, J., Morrel-Samuels, P. & Tao, F.-C. (2012), 'Player preferences among new and old violins.', *Proceedings of the National Academy of Sciences of the United States of America* **109**(3), 760–763.
URL: <http://www.pubmedcentral.nih.gov/articlerender.fcgi?artid=3271912tool=pmcentrezrendertype=abstract>
- 375 Glass Samuel V.; & Zelinka, S. L. (2010), 'Wood Handbook, Chapter 04: Moisture Relations and Physical Properties of Wood', *Wood handbook : wood as an engineering material* (GTR-190), 1–19.
URL: <http://www.treesearch.fs.fed.us/pubs/37428>
- Gough, C. (2013), Vibrational Modes of the Violin Family, in 'Proceedings of the Stockholm Music Acoustics Conference, SMAC 2013', pp. 66–74.
- 380 Guitard, D. & El Amri, F. (1987), 'Modèles prévisionnels de comportement élastique tridimensionnel pour les bois feuillus et les bois résineux', *Annales des sciences forestières* **44**(3), 335–358.
- Haines, D. W. (1980), 'On Musical Instrument Wood', *Journal of Catgut Acoustical Society* **33**, 19–23.
- Hutchins, C. M. & Voskuil, D. (1993), 'Mode tuning for the violin maker', *CAS J* **2**(4), 5–9.
- Jansson, E. V. & Barczewski, R. (2016), 'On the Violin Bridge-Hill - Comparison of Experimental
 385 Testing and FEM', *Vibrations in Physical Systems* **27**.
- Lev-Yadun, S. & Aloni, R. (1991), 'An Experimental Method of Inducing 'Hazel' Wood in *Pinus Halepensis* (Pinaceae)', *Iawa Bulletin* **12**(4), 445–451.
- Nia, H. T., Jain, A. D., Liu, Y., Alam, M.-R., Barnas, R. & Makris, N. C. (2015), 'The evolution of air resonance power efficiency in the violin and its ancestors', *Proc. R. soc. A* **471**(2175), 1–15.
 390 **URL:** <http://www.ncbi.nlm.nih.gov/pubmed/25792964>
- Nocetti, M. & Romagnoli, M. (2008), 'Seasonal cambial activity of spruce (*picea abies karst.*) with indented rings in the Paneveggio Forest (Trento, Italy)', *Acta Biologica Cracoviensia Series Botanica* **50**(2), 27–34.
- Ohtani, J., Fukazawa, K. & Fukumorita, T. (1987), 'SEM observations on indented rings', *IAWA
 395 Bull.(NS)* **8**(2), 1113–124.
URL: <http://kdb.keew.org/kdb/detailedresult.do?id=74126>
- Ono, T. (1996), 'Frequency responses of wood for musical instruments in relation to the vibrational properties.', *Journal of the Acoustical Society of Japan (E)* **17**(4), 183–193.
URL: <http://ci.nii.ac.jp/naid/130002033715/>
- 400 Racko, V. & Cunderlik, I. (2006), Selected Mechanical Properties of "Hazel Wood" in Norway Spruce (*Picea Abies L.*), in 'Wood Structure and Properties' 06', Arbora Publishers, Zvolen, pp. 369–371.
- Račko, V., Kačík, F., Mišíková, O., Hlaváč, P., Čunderlík, I. & Ďurkovič, J. (2018), 'The onset of
 405 hazel wood formation in Norway spruce (*Picea abies* [L .] Karst .) stems', *Annals of Forest Science* **75**(82), 1–11.
- Racko, V., Misikov, O. & Seman, B. (2014), Effect the Indentation of the Annual Growth Rings in Norway Spruce (*Picea Abies L .*) on Shear Strength - Preliminary Study, in 'Proceedings of the 57th International Convention of Society of Wood Science and Technology', number January, Zvolen.

410 Romagnoli, M., Bernabei, M. & Codipietro, G. (2003), 'Density variations in spruce wood with indented rings (*Picea abies karst*)', *Holz als Roh - und Werkstoff* **61**(4), 311–312.

Schindelin, J., Arganda-Carreras, I., Frise, E., Kaynig, V., Longair, M., Pietzsch, T., Preibisch, S., Rueden, C., Saalfeld, S., Schmid, B., Tinevez, J.-Y., White, D. J., Hartenstein, V., Eliceiri, K., Tomancak, P. & Cardona, A. (2012), 'Fiji: an open-source platform for biological-image analysis',
415 *Nature Methods* **9**(7), 676–682.
URL: <https://doi.org/10.1038/nmeth.2019>

Schweingruber, F. H. (2008), *Wood Structure and Environment*, Springer.

Sinclair, A. N. & Farshad, M. (1987), 'A comparison of three methods for determining elastic constants of wood', *journal of testing and evaluation* **15**(2), 77–86.

420 Viala, R. (2018), Towards a model-based decision support tool for stringed musical instrument making, PhD thesis, Université Bourgogne Franche-comté.
URL: <https://hal.archives-ouvertes.fr/tel-02877895>

Viala, R., Placet, V. & Cogan, S. (2019), 'Model-based quantification of the effect of wood modifications on the dynamics of the violin', *International Symposium on Music Acoustics, ISMA 2019*
425 (September).

Viala, R., Placet, V. & Cogan, S. (2020), 'Simultaneous non-destructive identification of multiple elastic and damping properties of spruce tonewood to improve grading', *Journal of Cultural Heritage* **42**, 108–116.
URL: <https://doi.org/10.1016/j.culher.2019.09.004>

430 Viala, R., Placet, V., Cogan, S. & Foltête, E. (2016), Model-based effects screening of stringed instruments, in 'Conference Proceedings of the Society for Experimental Mechanics Series', Vol. 3, pp. 151–157.

Wegst, U. G. K. (2006), 'Wood for sound', *American Journal of Botany* **93**(10), 1439–1448.

Woodhouse, J. (2005), 'On the Bridge-Hill of the Violin', *Acta acustica united with acustica* **91**(1), 155–165.
URL: <http://www.music.mcgill.ca/~gary/courses/projects/6182009/MahmoodMovassagh/MahmoodMovassaghProject.pdf>

435 Yaman, B. (2007), 'Anatomy of Lebanon cedar (*Cedrus libani* A. Rich.) wood with indented growth rings', *Acta Biologica Cracoviensia Series Botanica* **49**(1), 19–23.